

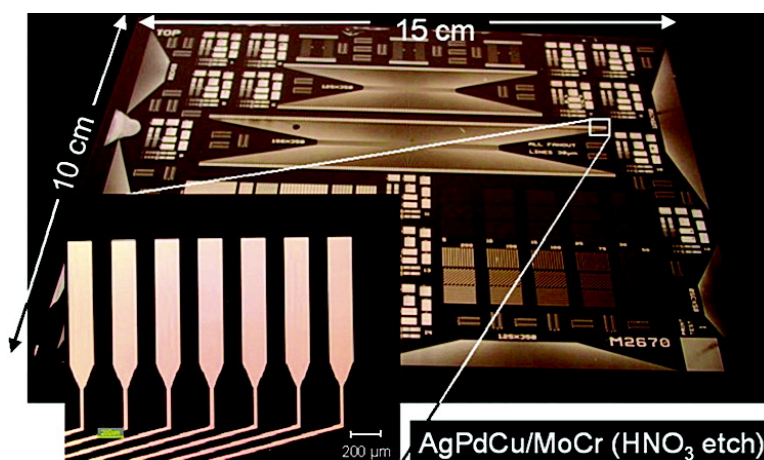
Communication

Single Etch Patterning of Stacked Silver and Molybdenum Alloy Layers on Glass Using Microcontact Wave Printing

Dirk Burdinski, Harold J. A. Brans, and Michel M. J. Decr

J. Am. Chem. Soc., **2005**, 127 (31), 10786-10787 • DOI: 10.1021/ja0523791 • Publication Date (Web): 13 July 2005

Downloaded from <http://pubs.acs.org> on March 25, 2009



More About This Article

Additional resources and features associated with this article are available within the HTML version:

- Supporting Information
- Links to the 4 articles that cite this article, as of the time of this article download
- Access to high resolution figures
- Links to articles and content related to this article
- Copyright permission to reproduce figures and/or text from this article

[View the Full Text HTML](#)

Single Etch Patterning of Stacked Silver and Molybdenum Alloy Layers on Glass Using Microcontact Wave Printing

Dirk Burdinski,^{*,†} Harold J. A. Brans,[‡] and Michel M. J. Decré[†]

Philips Research, Prof. Holstlaan 4, 5656 AA Eindhoven, The Netherlands, and Philips Applied Technologies, 5600 MD Eindhoven, The Netherlands

Received April 12, 2005; E-mail: dirk.burdinski@philips.com

Microcontact printing (μ CP), the archetype of modern soft lithographic patterning techniques, has undergone an impressive development over the past decade.¹ It has the potential for easy, fast, and cheap reproduction of structured surfaces and conductive layers with medium to high resolution (≥ 100 nm) even on curved substrates.² The commercial success of μ CP critically depends on realizing these promises in simple, cheap, and flexible large-area patterning processes. We have now developed a single etch step process for the patterning of TFT-LCD driver electrode structures comprising layers of silver and molybdenum alloys utilizing μ CP and HNO_3 -based etching employing SAM-stabilizing additives.

In μ CP a patterned self-assembled monolayer (SAM) of organic molecules is printed on the surface of a substrate with an elastomeric stamp. The SAM can be used as a resist to transcribe the pattern into underlying metal layers by etching. This has been demonstrated for various materials, including Au, Ag, Cu, Pd, and metal oxides typically on a laboratory scale. More recently, advanced μ CP schemes were developed to avoid problems associated with the up-scaling of these methods.³

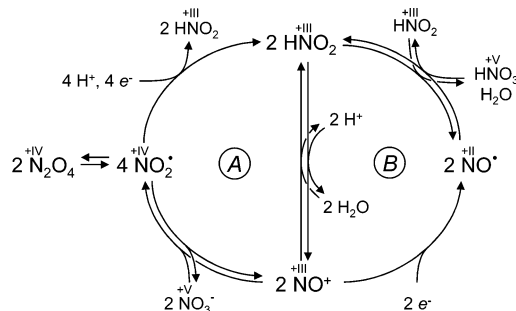
We have chosen a low resistivity silver alloy (98.1% Ag, 0.9% Pd, 1.0% Cu, APC, 200 nm thick, sputtered) on top of a molybdenum–chromium (97% Mo, 3% Cr, “MoCr”, 20 nm, sputtered) adhesion layer on glass substrates for the gate electrode layer of an active matrix LCD display design. A minimum number of process steps and etch defects can be obtained by direct patterning via μ CP of an alkanethiol SAM onto the top APC layer followed by single-step etching of both layers. Wave printing was used for stamping with regular PDMS stamps (Sylgard 184, 6 in.), which were inked with an octadecanethiol (ODT) ink solution (2 mM, ethanol). Wave printing enables μ CP on wafer-scale substrates with the required resolution and position control of better than 2 μm .⁴ The single-step development of printed test patterns, nevertheless, turned out to be challenging.

Mo or MoCr etching requires strongly acidic or alkaline etchants, due to the formation of passivating molybdenum oxide or polymolybdate layers,⁵ whereas for microcontact printed Ag patterns mild etchants are most suitable.⁶ In industrial processes nitric acid-based etchants are preferred although their etching mechanism is not well understood. HNO_3 -based etchants contain various strongly oxidizing species (e.g. NO^+ , NO_2^+ , NO_2^+), each of which can play a dominant role in the etching mechanism. Controlling the etch reaction is often difficult due to its autocatalytic character.



Nitrous acid, the initial reaction product (eq 1), equilibrates with NO^+ under strongly acidic conditions via protonation and dehydration (Scheme 1).⁷ The strong oxidizer NO^+ can initiate metal oxidation (cycle B) to form NO^* , which equilibrates with HNO_3

Scheme 1. Autocatalytic Reaction Cycles in HNO_3 -Based Etchants



and water to form HNO_2 .⁸ NO^+ can alternatively react with excess nitrate to form strongly oxidizing NO_2^+ , which turns into HNO_2 via an alternative metal oxidation route (cycle A).⁹ The production of more HNO_2 in each turnover accelerates the reaction. Since alkanethiol SAM resist layers (2–3 nm thick) are 2–3 orders of magnitude thinner than conventional photoresist layers (usually 0.2–2 μm thick), they are much more sensitive to such aggressive etching conditions. HNO_3 -based etchants have therefore been applied rarely to develop SAM patterned metal layers.¹⁰

When applied to APC/MoCr samples bearing a patterned ODT SAM, an optimized NPW (HNO_3 , H_3PO_4 , H_2O (3:9:13)) etchant provided reasonably structured small substrates (< 1 cm^2), but very inhomogeneous etching results when applied to larger substrates (10 \times 15 cm^2 , Figure S1). This is indicative of a strongly autocatalytic etching reaction, which also caused poor quality, particularly of larger features. The etch homogeneity was improved upon replacement of phosphoric acid by less viscous acetic acid and addition of sodium nitrite. The provided high initial nitrite concentration compensates for the lower etching rate and eliminates the autocatalytic effect.¹¹ The poor pattern quality, however, could only be improved by further substituting acetic acid with trifluoroacetic acid (TFA)(Figure S2). An optimized NTW (HNO_3 , TFA, H_2O (3:9:13); NaNO_2 (10^{-3} M)) etchant etched a 10 \times 15 cm^2 substrate homogeneously in approximately 150 s (Figure S3). A nitrite concentration of not less than 10^{-3} M was found to be indispensable for a homogeneous etching process (Figure S4).

We hypothesize that the higher acidity of TFA ($\text{p}K_a = 0.52$) compared to H_3PO_4 ($\text{p}K_{a,1} = 2.16$) and acetic acid ($\text{p}K_a = 4.76$) is important for the improved etch selectivity. A low concentration of deprotonated nitrate and a high ionic strength can shift the equilibrium between the two main oxidants NO^+ ($+ \text{NO}_3^-$) and NO_2^+ (Scheme 1) to the side of the charged species.¹² High NO^+ and NO_2^+ concentrations are characteristic of nitrous and nitric acid solutions in strongly acidic media, particularly in TFA.¹³ This equilibrium shift of the reactive species is considered important for the stability of the etch resist, since strongly hydrated NO^+ and NO_2^+ are less likely than neutral oxidizers, such as NO_2^* , to penetrate the hydrophobic ODT SAM.¹⁴ In fact, largely different SAM

[†] Philips Research.

[‡] Philips Applied Technologies.

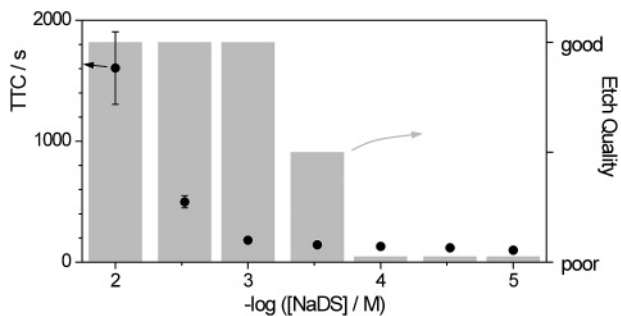


Figure 1. Time to clear (TTC) and etch quality for the complete etching of an APC/MoCr (200/20 nm) double layer with an NTW etchant (HNO_3 (65%), TFA (99%), H_2O (3:9:13); NaNO_2 (10^{-1} M)) as a function of the sodium decanesulfonate (NaDS) concentration (10^{-5} – 10^{-2} mol/L).

penetration capabilities were reported for similarly sized but differently charged metal complexes.¹⁵ Thus, for HNO_3 -based etchants the most acidic etching conditions unexpectedly appear to be least aggressive against the chosen SAM resist.

Despite the very homogeneous etch process, NTW-etched substrates still exhibited a significant number of etch defects. These are ascribed to molecular defects in the ODT layer, which result from impurities and the imperfect flatness of the sputtered APC layer and open a path for the etchant to reach the substrate surface. Saturation of the etchant with 1-octanol, which is known to induce a defect-healing effect in neutral and alkaline etching solutions, did not reduce the etch-defect density.¹⁶ This may be explained by oxidative octanol decomposition or a high degree of alcohol protonation in the acidic medium causing Coulombic repulsion. Therefore, the use of acidic surfactants that are uncharged, under low pH conditions, was considered. Monoalkyl sulfate esters were, however, believed to be insufficiently stable.¹⁷

The largest reduction of etch defects was observed upon addition of alkanesulfonates, $\text{H}(\text{CH}_2)_n\text{SO}_3^-$, with $n = 8$ – 12 , to the NTW etchant. For shorter alkyl chains defect reduction was insufficient, whereas for longer chains problems arose due to impractically long etching times and a low solubility.¹⁸ For $n > 7$ a steady increase of the time to clear (TTC) with the chain length was observed, probably due to the formation of increasingly stable alkanesulfonic acid SAMs on unmodified surface areas (Figure S5).¹⁶ For sodium decanesulfonate (NaDS, $n = 10$), the most suitable additive, a strong dependence of the etch performance on the concentration was found. In the NaDS concentration range below 3×10^{-4} M defect densities were high, whereas essentially no defects were observed at higher concentrations (Figure S6). Above 10^{-3} M, however, the advantage of defect reduction was counterbalanced by a dramatic reduction of the etching rate (Figure 1); hence, an NaDS concentration of 10^{-3} M is considered the optimum. A further increase of the nitrite concentration to 0.1 M could compensate for the generally somewhat reduced etching rates in the presence of the NaDS additive.

The thus further optimized NTW etchant (HNO_3 , TFA, H_2O (3:9:13); NaNO_2 (10^{-1} M); NaDS (10^{-3} M)) etched a 10×15 cm² microcontact wave printed APC/MoCr (200/20 nm) substrate homogeneously and essentially defect free in about 100 s (Figure 2).¹⁹ The maximum overetch was about $0.6 \mu\text{m}$, yielding fully conductive lines with a nominal width of $2 \mu\text{m}$ and a measured width of $0.8 \mu\text{m}$ (Figure S7), and electrically isolated ($R > 10^9 \Omega$) channels down to a measured width of $3 \mu\text{m}$. We have thus demonstrated single-etch patterning of stacked Mo and Ag alloys on a 10×15 cm² glass substrate using microcontact wave printing and an HNO_3 -based etchant, which marks an important step toward industrialization of microcontact printing.

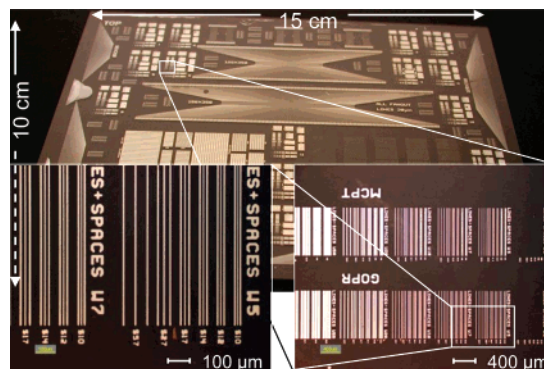


Figure 2. Optical micrographs of an APC/MoCr (200/20 nm) substrate (10×15 cm²) microcontact wave printed (ODT ink, AM-LCD test structures) and etched with an optimized NTW etchant (HNO_3 (65%), TFA (99%), H_2O (3:9:13); NaNO_2 (10^{-1} M)) containing NaDS (10^{-3} M) as a SAM-healing additive.

Acknowledgment. We are grateful to our colleagues, H. A. G. Nulens, C. J. Curling, and J. Chapman for their support.

Supporting Information Available: Figures S1–S7 and experimental details. This material is available free of charge via the Internet at <http://pubs.acs.org>.

References

- (a) Kumar, A.; Whitesides, G. M. *Appl. Phys. Lett.* **1993**, *63*, 2002–2004. (b) Smith, R. K.; Lewis, P. A.; Weiss, P. S. *Prog. Surf. Sci.* **2004**, *75*, 1–68. (c) Gates, B. D.; Xu, Q.; Love, J. C.; Wolfe, D. B.; Whitesides, G. M. *Annu. Rev. Mater. Res.* **2004**, *34*, 339–372. (d) Geissler, M.; Xia, Y. *Adv. Mater.* **2004**, *16*, 1249–1269.
- Jackman, R. J.; Wilbur, J. L.; Whitesides, G. M. *Science* **1995**, *269*, 664–666.
- (a) Rogers, J. A.; Bao, Z.; Baldwin, K.; Dodabalapur, A.; Crone, B.; Raju, V. R.; Kuck, V.; Katz, H.; Amundson, K.; Ewing, J.; Drzagic, P. *Proc. Natl. Acad. Sci. U.S.A.* **2001**, *98*, 4835–4840. (b) Delamarche, E.; Geissler, M.; Magnuson, R. H.; Schmid, H.; Michel, B. *Langmuir* **2003**, *19*, 5892–5897. (c) Geissler, M.; Kind, H.; Schmidt-Winkel, P.; Michel, B.; Delamarche, E. *Langmuir* **2003**, *19*, 6283–6296. (d) Delamarche, E.; Vichiconti, J.; Hall, S. A.; Geissler, M.; Graham, W.; Michel, B.; Nunes, R. *Langmuir* **2003**, *19*, 6567–6569.
- (a) Schellekens, J.; Burdinski, D.; Saalmink, M.; Beenhakkers, M.; Gelinck, G.; Decré, M. M. *J. Mater. Res. Soc. Symp. Proc.* **2004**, *EXS-2*, 21–23. (b) Decré, M. M. J.; Schneider, R.; Burdinski, D.; Schellekens, J.; Saalmink, M.; Dona, R. *Mater. Res. Soc. Symp. Proc.* **2004**, *EXS-2*, 59–61.
- Tsujimura, T.; Makita, A. *J. Vac. Sci. Technol., B* **2002**, *20*, 1907–1913.
- (a) Xia, Y.; Kim, E.; Whitesides, G. M. *J. Electrochem. Soc.* **1996**, *143*, 1070–1079. (b) Tate, J.; Rogers, J. A.; Jones, C. D. W.; Vyas, B.; Murphy, D. W.; Li, W.; Bao, Z.; Slusher, R. E.; Dodabalapur, A.; Katz, H. E. *Langmuir* **2000**, *16*, 6054–6060.
- Francisco, J. S. *J. Chem. Phys.* **2001**, *115*, 2117–2122.
- (a) Balbaud, F.; Sanchez, G.; Fauvet, P.; Santarini, G.; Picard, G. *Corros. Sci.* **2000**, *42*, 1685–1707. (b) Schmid, G.; Lobeck, M. A.; Keiser, H. *Ber. Bunsen-Ges. Phys. Chem.* **1972**, *76*, 151–157.
- Hsieh, H. F.; Yeh, C. C.; Shih, H. C. *J. Electrochem. Soc.* **1992**, *139*, 1897–1902.
- Goetting, L. B.; Deng, T.; Whitesides, G. M. *Langmuir* **1999**, *15*, 1182–1191.
- Hsieh, H. F.; Yeh, C. C.; Shih, H. C. *J. Electrochem. Soc.* **1992**, *139*, 380–385.
- (a) Boughriet, A.; Coumare, A.; Fischer, J. C.; Wartel, M. *J. Electroanal. Chem.* **1986**, *200*, 217–229. (b) Addison, C. C. *Chem. Rev.* **1980**, *80*, 21–39.
- (a) Turney, T. A.; Wright, G. A. *Chem. Rev.* **1959**, *59*, 497–513. (b) Spitzer, U. A.; Stewart, R. J. *Org. Chem.* **1974**, *39*, 3936–3937. (c) Beake, B. D.; Moodie, R. B. *J. Chem. Soc., Perkin Trans. 2* **1998**, 1–5.
- Porter, M. D.; Bright, T. B.; Allara, D. L.; Chidsey, C. E. D. *J. Am. Chem. Soc.* **1987**, *109*, 3559–3568.
- (a) French, M.; Creager, S. E. *Langmuir* **1998**, *14*, 2129–2133. (b) Becka, A. M.; Miller, C. J. *J. Phys. Chem.* **1993**, *97*, 6233–6239.
- Geissler, M.; Schmid, H.; Bietsch, A.; Michel, B.; Delamarche, E. *Langmuir* **2002**, *18*, 2374–2377.
- Ward, R. N.; Davies, P. B.; Bain, C. D. *J. Phys. Chem. B* **1997**, *101*, 1594–1601.
- Creager, S. E.; Rowe, G. K. *Langmuir* **1993**, *9*, 2330–2336.
- Individual etch rates are reported in the Supporting Information.

JA0523791